Resistance anomaly and excess voltage in inhomogeneous superconducting aluminum thin films

M. Park,* M. S. Isaacson, and J. M. Parpia
School of Applied and Engineering Physics, and Laboratory of Atomic and Solid State Physics, Cornell University, Ithaca, New York 14853-2501

(Received 13 June 1996; revised manuscript received 18 December 1996)

We report measurements of the resistance and the current-voltage characteristics of aluminum thin films which have two regions of different superconducting transition temperatures. Local suppression of the transition temperature is achieved by the use of a CF_4 reactive ion-etching technique. A small gradient in the transition temperature is induced around the lithographically defined etched-unetched interface. As the temperature is increased from the superconducting state, we observe voltage (and hence resistance) increases above the normal-state value when measured with superconducting voltage probes located within $\sim$20 μm on either side of the interface. The excess voltage persists over a range of bias currents above I_C and eventually disappears, approaching the normal-state value at high bias currents. In an experiment where there are multiple voltage probes arranged along the film, the excess voltage is eliminated in steps with increasing bias current, resulting in a series of negative differential resistance peaks. These unusual phenomena are explained by a nonequilibrium charge imbalance model which requires the spatial dependences of the quasiparticle and pair electrochemical potentials to be different near normal-superconducting interfaces and phase-slip centers. We also report the observation of an asymmetry in the current-voltage characteristics which cannot be understood in terms of the nonequilibrium model. [S0163-1829(97)03814-9]

I. INTRODUCTION

Recently, an anomalous increase in the resistance above the normal-state value (R_N) has been observed near the superconducting transition in a wide variety of systems.[1–13] These systems range from one dimensional (1D) to bulk samples, conventional to compound superconductors, and single component to multicomponent systems. Due to the diversity in sample configurations and material properties, it is unclear how (and if) the various observations are connected to each other. Even though several different explanations for the anomaly have been proposed, its physical origin is still not well understood and the question whether there is a common physical origin for all these manifestations remains open. In this paper, we present a comprehensive study of such an anomaly in two-dimensional (2D) aluminum thin films. An abbreviated description and explanation of the experimental data are presented in our recent publication.[13] Here we present a detailed description of the data as well as a more complete discussion than that reported earlier. Throughout the paper, in discussing the different regions of the superconducting film, we follow the nomenclature of Yu and Mercereau.[14] A normal metal (N) refers to a superconductor at temperatures above its superconducting transition temperature (T_c), and a weak superconductor (W) refers to a superconductor dynamically driven with a dc bias current larger than its critical current (I_c).

Kwong *et al.*[1] explain that the resistance anomaly observed in their 2D aluminum system is due to differences between the nonequilibrium quasiparticle and pair electrochemical potentials in the superconductor near the normal-superconducting (NS) interface (the nonequilibrium charge imbalance model). However, the nonequilibrium nature of the anomaly was not fully explored, and consequently more experimental evidence which clearly explores the mechanism of the anomaly was needed. This prompted us to carry out further transport measurements on aluminum film structures and study in detail the behavior of the resistance data (R vs T) as well as the current-voltage (I-V) characteristics.

In the R vs T measurements in our 2D aluminum systems incorporating a NS interface, the resistance anomaly is observed only with S probes. We also report related anomalous I-V characteristics associated with the presence of phase-slip centers (PSC's) in the W region.[13] With increasing dc bias current the voltage rises to above the normal-state value (IR_N) before it eventually approaches the usual normal-state I-V characteristics at higher biases. The excess voltage decreases in steps manifested as a series of negative differential resistance (dV/dI) peaks. This incremental decrease of the excess voltage is a nonlocal effect. We have proposed an explanation[13] that the I-V characteristics are modified by the presence of PSC's whose locations and interactions are influenced by the sample inhomogeneity and voltage probes $\sim$10 μm farther down the conduction path from the region that is sampled. We find that the nonequilibrium charge imbalance model successfully explains the major features of the anomaly in our aluminum films. The different spatial dependences of the quasiparticle and pair electrochemical potentials which exist in the nonequilibrium region near NS interfaces and PSC's are necessary to understand the behaviors of the R vs T data and I-V characteristics. The spatial extent of this nonequilibrium region is accentuated due to long quasiparticle relaxation times in our aluminum films.

In this paper, after first describing the samples and experimental details, we will discuss the main features of the resistance anomaly in the R vs T data and the I-V characteristics within the nonequilibrium charge imbalance model. In our discussion of the I-V characteristics (of the current driven W region), we will first consider a heuristic picture which is a direct extension of the charge imbalance model

0163-1829/97/55(14)/9067(10)/$10.00

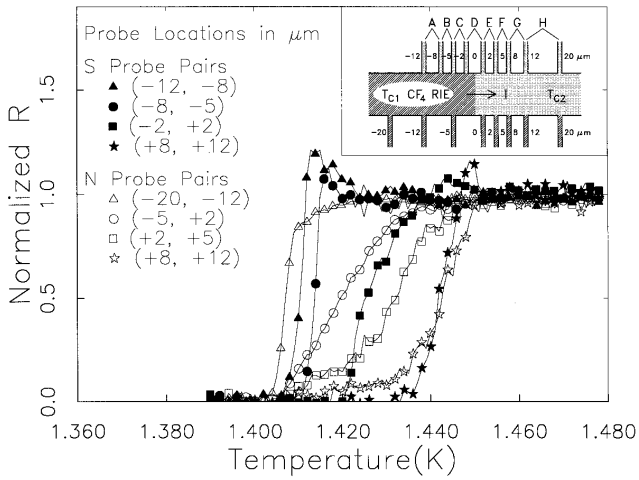

FIG. 1. Resistive transitions of several sections near the etched-unetched interface at zero-bias current. The curves plotted with filled symbols show the transitions measured with S (unetched) probes and the open symbols N (etched) probes. With S probes the resistance anomaly is observed in all the sections. With N probes, no resistance anomaly is observed. Inset: The top view of the aluminum film structure with multiple voltage probes at various distances from the etched-unetched interface. A, B, . . . , and H refer to sections between the probes. The hashed areas represent the regions where the T_c is suppressed. The interface is designated as the origin; negative positions represent the etched region and the positive positions the unetched region. Each voltage probe is marked with the distance (in μm) of its inner edge from the interface.

presented as the explanation for the resistance anomaly in the R vs T data (of the zero-biased case). We will finally focus on the explanation of the excess voltage in the I-V characteristics and its incremental decrease with increasing dc bias current in terms of the PSC model.[13] An observed asymmetry in the I-V characteristics with the current bias direction will be also included in the paper.

II. THE SAMPLES AND EXPERIMENTAL DETAILS

Two aluminum film structures will be discussed in this paper. Schematics of the structures are shown in the insets in Figs. 1 and 11. For both structures, the aluminum film and voltage probes are lithographically patterned as a single continuous film. The details of the fabrication are given elsewhere.[15] The T_c of the region on the left in each structure is suppressed by the use of a CF_4 reactive ion-etching (RIE) technique. The RIE exposure depletes the surface oxygen in the aluminum film, suppressing T_c by a few percent in the hashed regions. The normal-state properties are largely unaffected and remain almost identical.[15] The sharpness of the lithographically defined etched-unetched interface appears to be $\sim$0.1 μm or better.[16] N probes in the inset in Fig. 1 are created by the same process. The thickness and width of the films are 250 Å and 20 μm, respectively, and the width of the voltage probes is 1 μm.

Tunnel junctions are preferred as a means of measuring potentials since their use minimizes the effect of voltage probes on the system. However, due to difficulties in fabrication of such junctions and in particular their integration with our etch process, we used narrow side voltage probes patterned as a continuous film (insets in Figs. 1 and 11). Such side voltage probes have been used in the past.[1,2,14,17] S probes will measure the pair electrochemical potential and N probes will measure the quasiparticle electrochemical potential.[18] The presence of these probes does locally shift T_c via the proximity effect over a length scale of the coherence length, $\xi(T)\sim 1$ μm. This is small compared to the film width, and the excess voltage and resistance anomaly are not due to the use of the side voltage probes.[19]

In the inset in Fig. 1, multiple voltage probes (both N and S) are located at various distances from the etched-unetched interface. In the inset in Fig. 11, only a single pair of S voltage probes is located near the interface. The main discussion of the paper will concentrate on the experimental results obtained in the structure with multiple probes, shown in the inset in Fig. 1. The results from the structure with a single pair of probes shown in the inset of Fig. 11 will be presented in comparison with the multiple probe case in Sec. IV D.

For the film with multiple probes described in this paper, $T_{c1}=1.407$ K and $T_{c2}=1.452$ K where T_{c1} and T_{c2} refer to the T_c's of the etched and unetched regions far away from the interface. For both etched and unetched regions, the normal-state resistivity, diffusion constant, and elastic mean free path are $\sim 2\mu\Omega$ cm, $\sim$40 cm^2/s, and $\sim$100 Å, respectively. The residual resistance ratio is $\sim$2.2; and $\xi(T)$ is $\sim 1\mu$m for the dV/dI curves reported here. The second sample with a single pair of probes has slightly different film properties (somewhat cleaner)[20] since it was prepared in a separate fabrication.

The samples are cooled down in a ^{4}He cryostat and the thermometry is achieved by monitoring the resistance of a calibrated germanium sensor. Standard four-terminal measurements are carried out in the earth's magnetic field using a lock-in amplifier with a small ac signal of 0.2 μA (producing a current density of 40 A/cm^2 at 101 Hz). The R vs T data are measured at zero dc bias current while sweeping the temperature. The differential resistance (dV/dI vs I) is measured at a fixed temperature with an increasing dc bias current on which the same small ac modulation is superimposed. The I-V characteristics are obtained by integrating dV/dI instead of a direct dc measurement in order to gain a better signal-to-noise ratio. (Similar, though less precise, results are observed by dc techniques.) There is negligible hysteresis except at very high currents ($>$70 μA). This is important since it is an indication that the phenomena which we present here are not related to self-heating.

III. RESISTANCE ANOMALY

A. Resistance peak in *R* vs *T*

In Fig. 1, we present the R vs T data which are measured with pairs of either S (unetched) or N (etched) voltage probes which are located near the etched-unetched interface and as well as those which span the interface. When $T_{c1}<T<T_{c2}$, a NS interface is present in the film, and the etched probes are normal whereas the unetched probes are superconducting. In all the sections of the film within $\sim\pm 20$ μm from the etched-unetched interface, the anomalous resistance peak above R_N is observed in the vicinity of the transition only with S voltage probes. (For clarity, only several transitions are plotted in the figure as examples.) This

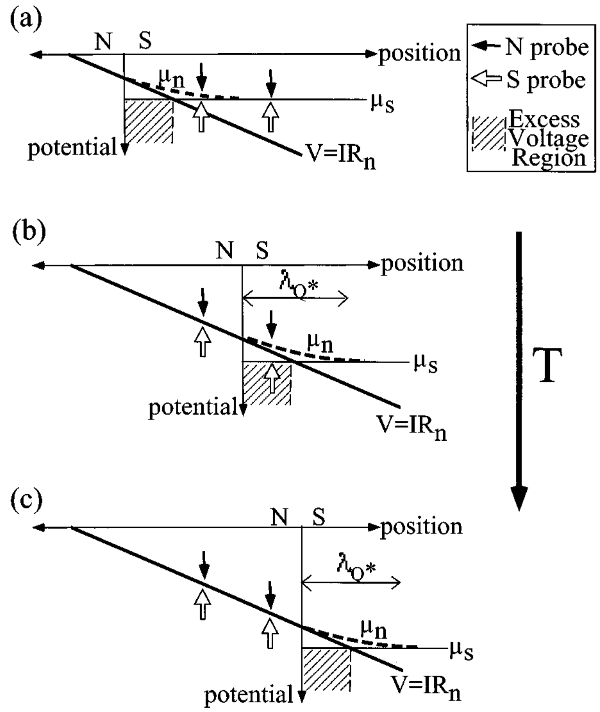

FIG. 2. Spatial dependences of the potentials around a NS interface. (a), (b), and (c) illustrate a simple model for the NS interface traversing the film when the temperature is increased. In a superconductor, the quasiparticle electrochemical potential (thick dashed line) decays toward the constant pair electrochemical potential (thin solid line) over a distance of λ_{Q*}, as shown in (b) and (c). [In (a), λ_{Q*} is not marked due to the crowded space.] The normal-state potential (thick solid line) is linear with position and drawn assuming the same resistivity for both *N* and *S* sides. The hatched region represents the possible locations of the second *S* voltage probe which would measure an excess voltage if the other probe were located on the *N* side. This region is referred as ''the excess voltage region'' in this paper. (a) At temperatures below local T_c, *S* probes measure a zero voltage difference, whereas *N* probes start to measure a finite voltage even before the interface moves between the probes due to a long quasiparticle electrochemical potential tail in the *S* region. (b) Once the interface moves in between the probes, *S* probes measure an excess voltage, a potential difference larger than the normal-state value, whereas *N* probes measure the smaller quasiparticle value. (c) At high temperatures above the local T_c, the interface has moved out of the sampled region, and both *S* and *N* probes measure the normal-state value.

resistance anomaly is also reflected in the *I*-*V* measurements, described later in the paper. (See also Fig. 3 in our previous publication.[13]) This confirms that our observation of the resistance anomaly in the *R* vs *T* data is a true resistance increase and not an artifact of the ac measurement technique.

B. Nonequilibrium charge imbalance model

When a current flows into a superconducting interface from a normal metal, the quasiparticle distribution is driven out of thermal equilibrium. This leads to a charge imbalance between the hole and electron like branches of the quasiparticle excitations.[21] In the superconductor near a NS interface, a nonequilibrium region develops where the quasiparticles and Cooper pairs have different spatial gradients of their respective electrochemical potentials (see Fig. 2). The differences between the potentials have been directly measured near NS interfaces,[14] using both *S* and *N* voltage probes for the pair and quasiparticle electrochemical potentials, respectively.

A pair of *S* voltage probes located around a NS interface samples a potential gradient which exceeds the normal-state potential gradient that the *S* side would exhibit if it were in its normal state. See Fig. 2(b). [For now, we will concentrate only on Fig. 2(b). A complete discussion of the figure including (a) and (c) will be given in Sec. III D.] This excessive potential gradient is due to the nearly constant pair electrochemical potential.[1] Thus, an excess voltage and resistance are measured with *S* probes around a NS interface. For example, a pair of *S* probes around the etched-unetched interface such as ones located at -2 and 2 μm registers the resistance anomaly (Fig. 1). However, *N* probes do not measure this excess voltage (hence, no resistance anomaly) since they measure the spatial gradient in the quasiparticle electrochemical potential which never exceeds the normal-state value [Fig. 2(b)]. A more detailed discussion of the anomaly will be presented in Sec. III D that follows.

The spatial extent of ''the excess voltage region,'' which is defined in Fig. 2, is determined by the quasiparticle charge relaxation processes and the resistivity of the superconducting film. In aluminum the relaxation length λ_{Q*} is long and the resistivity is low. In our film, the estimated λ_{Q*} is $\sim$10–20 μm at $T=1.390$ K with the inelastic-scattering time (at T_c and Fermi energy) of $\sim$10–40 ns, assuming that inelastic-scattering events provide the dominant relaxation process.[21–24] The enhancement of the relaxation lengths due to the proximity to T_c makes our aluminum film particularly favorable for measurements of the nonequilibrium behavior.

Even though the existence of the nonequilibrium quasiparticle and pair electrochemical potentials near superconducting interfaces has been investigated both theoretically and experimentally for about 20 years,[21] it has only recently manifested as a resistance anomaly. For example, in the case of a single NS interface, the increase in the resistance above the normal-state value results only when one of the sampling *S* voltage probes spanning the interface is located within the excess voltage region (see Fig. 2). If the second *S* probe is located deep within the *S* region, it will measure a resistance due to the *N* side and the contribution from the nonequilibrium region (proportional to λ_{Q*}). However this resistance will not exceed the total normal-state value of both the *N* and *S* regions (see Fig. 2). With the use of the recently developed film fabrication technique, one is able to routinely produce structures with narrow probes located close enough to the interface so as to be within the excess voltage region. Also, even if the second probe is located close to the interface, it is difficult to resolve the anomalous excess in resistance when the normal-state resistance of the *N* side is very large compared to the nonequilibrium portion. The anomaly is also difficult to resolve when the nonequilibrium region is diminished due to a short λ_{Q*}. Our fabricated aluminum film structures with a T_c shifted by RIE exposure[15] have a long λ_{Q*} and low resistivity, and are thus more likely to provide favorable conditions for the observation of the anomaly.

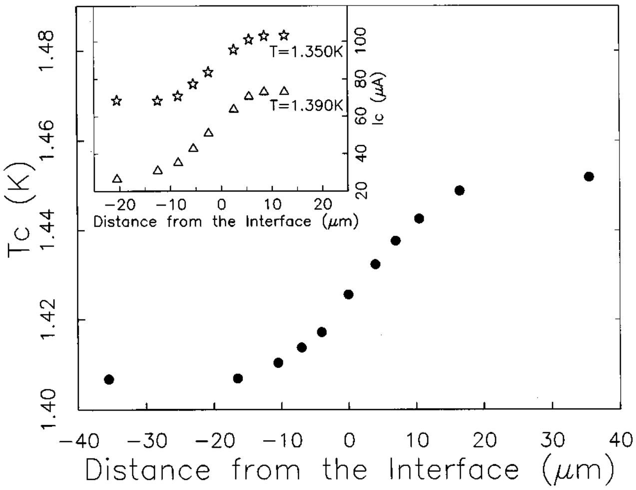

FIG. 3. Spatial variation of T_c near the etched-unetched interface. Inset: Spatial variation of I_c near the etched-unetched interface. Each curve corresponds to a different temperature, and both temperatures are below T_{c1}.

C. Inhomogeneity induced around the etched-unetched interface

Figure 3 shows the inhomogeneity in the superconducting properties induced by the presence of the etched-unetched interface in the aluminum film. It demonstrates the gradual variation of the superconducting order parameter in our film. Figure 3 shows the spatial variation of the T_c. Far away (on both sides) from the etched-unetched interface, the film has a constant T_c (T_{c1} or T_{c2}). The transition temperature varies from T_{c1} to T_{c2} over a length scale $\sim\pm 20$ μm around the interface. We note that this length scale is much larger than the characteristic length scale of the proximity effect,[25] which is estimated to be $\sim 1\mu$m or less in our film. The variation of T_c over a long range around the etched-unetched interface in our film is consistent with the previously reported observation in a similarly fabricated aluminum film structure with periodically modulated T_c.[26] It was observed that the system exhibits a single homogeneous transition for modulation lengths up to ~ 50 μm.[27] In Fig. 3, the points in the figure are obtained from a set of R vs T measurements at zero-bias current using adjacent pairs of voltage probes located near the etched-unetched interface (see the inset in Fig. 1). The T_c is chosen to be the temperature at which the resistance falls to one half of the normal-state value. The positions are the mean locations of the voltage probes.

As expected, in the inset of Fig. 3, the I_c of the film shows a spatial dependence similar to that of the T_c. The etched side has a lower I_c corresponding to its lower T_c compared to the unetched side. The constant I_c values far away from the etched-unetched interface on both sides are referred as I_{c1} and I_{c2} in the paper. The points in the curves in the inset are obtained by measuring a set of I-V characteristics of the sections between the adjacent probes, sections A–H (see the inset in Fig. 1), at two fixed temperatures below T_{c1}. We define the I_c to be the value of the current at the maximum in dV/dI, obtained from measurements which will be described later in this paper.

D. Motion of the NS interface and anomaly in *R* vs *T*: The simple model

From the spatial dependence of T_c in Fig. 3, one can determine the location of the NS interface at a given temperature and at zero-bias current. When the temperature is below T_{c1}, the entire film is in its S state. As the temperature is increased, more of the film's area becomes normal. Hence, as the temperature is swept from $T<T_{c1}$ to $T>T_{c2}$, the NS interface transverses the film from the left to the right of the etched-unetched interface, through sections A–H. Eventually, the entire film is in its N state when the temperature is above T_{c2}.

Therefore, as the temperature is increased, one can picture the NS interface with the nonequilibrium potentials propagating along the film, as modeled in Fig. 2.[28] A pair of S voltage probes located within the region of varying T_c ($\sim\pm 20$ μm from the etched-unetched interface) first measures zero resistance at low temperatures since both probes measure the constant pair electrochemical potential [Fig. 2(a)]. When the temperature exceeds the T_c of the section to the left of the sampling probes, the NS interface moves between the probes and the resistance rapidly rises to a finite value. As the excess voltage region (defined as where the Ohmic potential line crosses the constant pair potential in Fig. 2) passes by the second S probe, a potential difference larger than the normal-state value is measured [Fig. 2(b)]. This excess voltage is manifested as the resistance anomaly. Since the length of the film spanned by each pair of adjacent probes is short compared to λ_{Q*} in our sample, the measured resistance with adjacent S probes quickly increases above the normal-state value once the NS interface moves in between the probes. With a further increase in temperature, the NS interface moves out of the sampled region, and the voltage probes (both being now in the N region) measure the normal-state resistance value [Fig. 2(c)].

According to this picture of the moving NS interface, the sampling probes need not span the etched-unetched interface in order to observe the anomaly, as long as they are superconducting and located within ~ 20 μm of the etched-unetched interface. Thus, in Fig. 1, the resistance anomaly is observed not only with S probes located around the etched-unetched interface but also with other pairs of S probes (see the curves plotted with the filled symbols). In contrast, the anomaly cannot be manifested using N probes (see the curves plotted with open symbols) since they measure the quasiparticle potential gradient which never exceeds the normal-state value [see Fig. 2(b)]. Instead, N probes start to measure a finite resistance value even before the NS interface moves in between the probes since they sample the quasiparticle electrochemical potential which has a long tail inside the S region [see Fig. 2(a)]. Thus, the resistive transitions measured with N probes appear to be more gradual than with S probes, as seen in Fig. 1 (compare the curves plotted with the filled and open symbols). The first curve (Δ) shows a sharp transition even though it is measured with N voltage probes since the probes are located farther inside the etched region where the film has a nearly constant T_c. The nonequilibrium picture of Fig. 2 of the moving NS interface correctly models the anomalous resistance peak as well as the shape of the resistive transitions in the R vs T data.

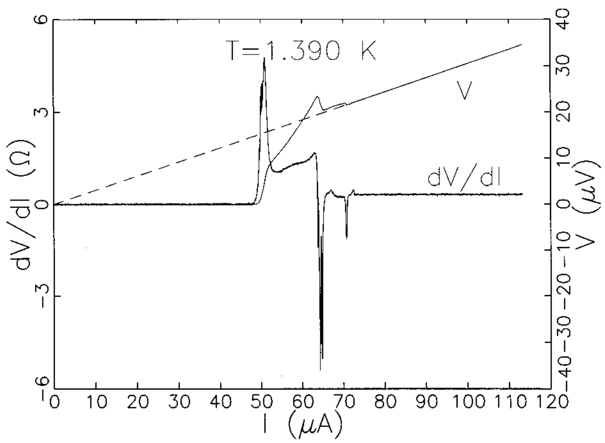

FIG. 4. Anomalous behavior of the differential resistance (left axis) and *I*-*V* characteristics (right axis) with a current bias at $T=1.390$ K. The voltage probes are superconducting and located at -2 and 2 μm from the etched-unetched interface. The dashed line is the normal-state *I*-*V* characteristics.

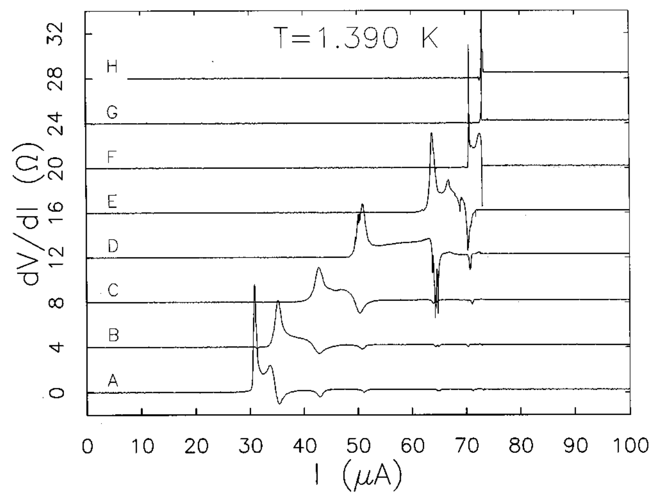

FIG. 5. The dV/dI's are measured across the sections A–H using pairs of adjacent S voltage probes at $T=1.390$ K. Each trace is shifted for comparison. Trace A corresponds to the measurement across the section A, trace B across the section B, and so on.

IV. EXPERIMENTS UNDER CURRENT BIAS

A. Anomaly in *I*-*V* characteristics

The *I*-*V* characteristics in Fig. 4 also show an anomaly (a region of excess voltage), measured with S probes at -2 and 2 μm at $T=1.390$ K. These measurements are qualitatively consistent with the R vs T data described in the previous section. For the current biased case, both etched and unetched probes are superconducting since the measurements are performed at temperatures below T_{c1} and T_{c2}, and the probes will register the pair electrochemical potential.[29] When I_c is exceeded, a voltage develops rapidly and increases to above IR_N before it approaches the normal-state Ohmic behavior. Furthermore, an interesting feature is visible on close examination of the *I*-*V* characteristics. The excess voltage persists over a range of currents above I_c and decreases in two steps which are manifested as negative dV/dI peaks. This feature will be discussed in Secs. IV C and IV D.

B. Extension of the simple model to the current biased system

In this section, we present a heuristic model in which we relate the observed anomaly in *I*-*V* characteristics to the spatial variation of the quasiparticle and pair electrochemical potentials in the W and S regions. In the current driven case, given the spatial gradient of I_c in the inset of Fig. 3 together with the simple picture of the moving interface as in Fig. 2, one can picture that a WS interface (instead of a NS interface) traverses the film from left to right as the current (instead of the temperature) is increased. The inset in Fig. 3 indicates the location of the WS interface along the film as the bias current is increased at a fixed temperature. As the current is increased, a larger portion of the film is driven out of the S state, and the WS interface moves through sections A–F. To the right of section F, the film has a nearly constant I_c. Once the current reaches the constant I_c value, the rest of the film is driven out of the S state nearly instantaneously.

The main features of the *I*-*V* characteristics in Fig. 4 can be understood with this simple picture of the moving WS interface. At low currents, the S probes measure a zero potential difference [analogous to Fig. 2(a)]. When the current is increased above the I_c of the section to the left of the probes, the WS interface moves in between the probes and a finite voltage is measured. As the excess voltage region passes by the second S probe, an excess voltage is measured [analogous to Fig. 2(b)]. With a further increase in the current, the WS interface moves to the right of the sampled region and the excess voltage is abruptly eliminated resulting in a negative dV/dI peak. At high currents, the measured voltage should show Ohmic behavior [analogous to Fig. 2(c)].

Figure 5 shows the dV/dI's of sections A–H. [For the corresponding *I*-*V* characteristics, see Fig. 5(b) in Ref. 13.] They qualitatively support the heuristic picture of the moving WS interface. The excess voltage peaks are observed consecutively in sections A–F as the bias current is increased. In trace A, when the WS interface moves past the first probe at -12 μm, a positive dV/dI peak is observed (at ~ 30 μA), indicating a rapid development of a finite voltage as the interface moves into section A. As the excess voltage region moves by the second probe at -8 μm, an excess voltage [see Fig. 5(b) in Ref. 13] is measured. When the WS interface moves past the second probe, a negative dV/dI peak is observed (at ~ 35 μA). At this same bias current, a positive dV/dI peak is observed in trace B indicating that the WS interface has now moved into section B. This sequential behavior is repeated until the bias current approaches the spatially constant value of I_c (I_{c2}) in the region far from the etched-unetched interface (see the inset in Fig. 3). At this high current, the remainder of the film is driven normal simultaneously; hence, neither an excess voltage or negative dV/dI peak is observed (traces G and H).

We have demonstrated that the simple model of the nonequilibrium charge imbalance near NS and WS interfaces successfully explains the main features of the R vs T data measured with S or N voltage probes, and qualitatively explains the *I*-*V* characteristics measured with S voltage probes. The experimental results are consistent with the con-

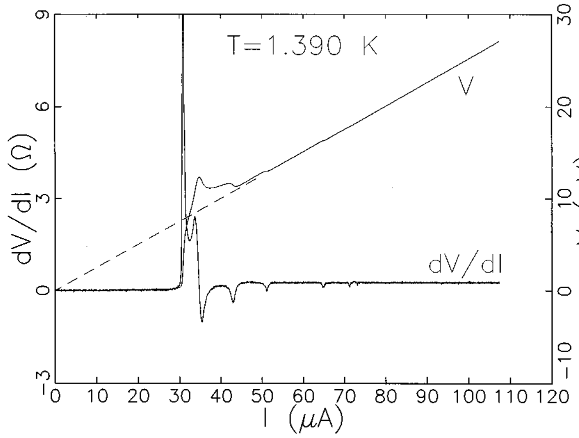

FIG. 6. The dV/dI's (left axis) and I-V (right axis) characteristics of section A at $T=1.390$ K. (It is the dV/dI and I-V characteristics of the section between the S probes located at -12 and -8 μm.) Note the persisting excess voltage and its incremental decrease. The dashed line is the normal-state I-V characteristics.

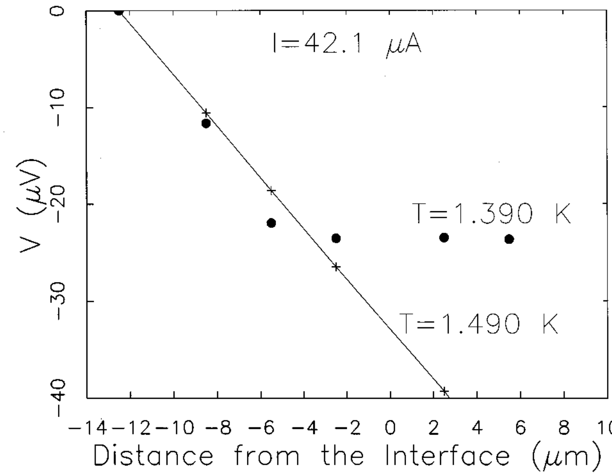

FIG. 7. The filled circles are the measured spatial dependence of potentials around the WS interface with S probes at a temperature below T_{c1}, and a current between I_{c1} and I_{c2}. The crosses are the measured spatial dependence of potentials at the same current but at a temperature above both T_{c1} and T_{c2}, (i.e., at the normal state). At $T=1.390$ K and $I=42.1$ μA, the WS interface is located between -3 and -6 μm (roughly at -5 μm from the inset in Fig. 3). The W region is to the left of the WS interface and the S region to the right. Note that the pair electrochemical potential does not revert to the normal-state potential in the W region.

clusion that the origin of the excess voltage (and hence the resistance anomaly) is the different spatial gradients of the quasiparticle and pair electrochemical potentials in the nonequilibrium S region.

C. Disagreement of the data with the simple model

Now we examine the I-V characteristics in Figs. 4 and 5 more closely, and point out the unexpected detailed features which disagree with the simple model presented in the previous section. In Fig. 4, most of the excess voltage is eliminated at a bias current value of ~65 μA. However, a small amount of excess voltage persists until the current is increased to ~70 μA. In Fig. 5, we note that traces A, B, C, and D show a series of smaller negative dV/dI peaks following the first negative peak which reflects the voltage reverting to that of the quasiparticles as the WS interface leaves the sampled region. The simple model gives no explanation for these features.

In order to emphasize the disagreement, trace A in Fig. 5 is replotted in Fig. 6. The excess voltage persists over a range of bias currents before the voltage reverts to the usual normal-state Ohmic behavior. The excess voltage is present even at currents up to ~40 μA above the current at which the WS interface moves out of the sampled section A (~35 μA). Moreover, the excess voltage decreases in steps which are manifested as a series of negative dV/dI peaks. Similar behavior is seen in other traces in Figs. 4 and 5. By comparing the current values of the dV/dI peaks in traces A–H in Fig. 5, it is apparent that these peaks occur whenever the WS interface moves by the locations of other probes which can be as far as ~16 μm away from the sampled region. If a section is completely driven to a normal state by the applied dc current it should not be affected by a change in the potential which occurs away from the sampled region as the WS interface passes by a distant section. The heuristic picture of a moving WS interface (analogous to that of NS interface as in Fig. 2) with nonequilibrium potential gradients existing only on the S side gives no simple explanation for the persistent excess voltage and nonlocal negative dV/dI peaks. According to this simple picture, once the WS interface moves through the pair of the sampling voltage probes, all of the excess voltage should be eliminated, producing a single negative dV/dI peak and reverting to the normal-state I-V characteristics at once. The data show a departure from this predicted behavior.

In a superconductor above its T_c, the pair electrochemical potential has no meaning. The spatial dependence of the potential is just that of the normal electrons and the linear Ohmic behavior drawn in Fig. 2 correctly models the potential inside the N region. Inside the dynamically driven W region at high currents, where all the current is carried by the quasiparticles, this picture also correctly represents the spatial dependence of the potential. However, inside the W region near T_c and at bias currents above but close to I_c, the order parameter is not yet zero. Generally, there are time and spatially dependent pairing and depairing interactions such as phase-slip centers,[30] and the simple Ohmic behavior alone inadequately represents the complex dynamics of the quasiparticles and pairs. In Fig. 7, we plot the measured spatial dependence of the pair electrochemical potential at a fixed current value, which can be inferred from a set of the measurements of the I-V characteristics obtained with S probes. The data implies that in the W region the pair electrochemical potential does not follow the normal-state dependence. Instead, they show a larger gradient than the normal-state potential and appear to vary spatially so as to rejoin the constant pair electrochemical potential in the S region. This behavior indicates a nonequilibrium between the pair and quasiparticle electrochemical potentials in the W region.

One explanation for the existence of such a spatial variation would be a smooth change in the pair electrochemical potential mapped by a line joining the filled circles in Fig. 7. Such a variation, together with the simple picture of the

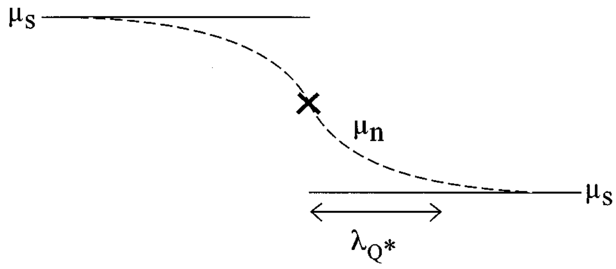

FIG. 8. Potentials near a single phase-slip center. The pair electrochemical potential is constant on both sides of a PSC, and the quasiparticle electrochemical potential exponentially decays toward the pair electrochemical potential over a distance λ_{Q*} from the center of the PSC.

moving WS interface as discussed in the previous section, would explain the persistent excess voltage. Still it would not produce the nonlocal negative dV/dI peaks (i.e., incremental decreases of the voltage). Negative peaks would result if the WS interface were to propagate abruptly to the right with increasing bias current. Such an abrupt motion is possible due to the presence of the S voltage probes which carry no current. Their presence will locally enhance the critical current and therefore momentarily prevent the motion of the interface as the current is swept.

However, a smooth spatial variation of the pair electrochemical potential is inconsistent with the present understanding of voltage sustaining current driven superconductors. In such a system, phase-slip centers are generally nucleated at regions of reduced critical current.[31,32] PSC's produce discrete changes in the potential[32,33] rather than the smoothly varying potential as we have inferred from Fig. 7 in the above discussion. In fact, the spatial variation of the pair electrochemical potential across a PSC occurs over a length scale of $\xi(\sim 1\ \mu\text{m})$ which is smaller than the probe spacing in our film (see the inset in Fig. 1). Thus, it is likely that the potential measurements shown in Fig. 7 do not have the resolution to reflect the rapid variation in the pair electrochemical potential. The interpretation of the potentials in Fig. 7 in terms of PSC's provides a more precise description for the experimental observations. In the following section, the model involving PSC's, which was also presented in the previous work,[13] will be discussed in detail, and we will show that the PSC description is consistent with the data and explains successfully the detailed features of the I-V characteristics.

D. Phase-slip center model, excess voltage, nonlocal effect

The potential variation around a single phase-slip center is particularly simple.[32,33] The time-averaged pair electrochemical potentials are constant on both sides of a PSC, but there is a discontinuity at the PSC itself. At a PSC, the order parameter undergoes a rapid oscillation generating excited quasiparticles which diffuse into the adjacent superconducting regions. In Fig. 8 we show the spatial variation of the electrochemical potentials in the vicinity of an isolated PSC. For our discussion we can treat the PSC as a normal core with S regions on either side. The pair and quasiparticle electrochemical potentials would show the same nonequilibrium behavior as in the case of a NS interface previously discussed in Sec. III B, but now extending a distance λ_{Q*} on either side of the PSC. Referring to Fig. 8, we note that S probes around a single PSC would register a voltage drop, $I_n\rho(2\lambda_{Q*})$, where I_n is the averaged normal current at the center of the PSC and ρ is the normal resistance per unit length. The spatial variation of the pair and quasiparticle electrochemical potentials are normally measured in 1D systems.[33] In our case, the PSC description is valid because of the long quasiparticle relaxation length, which is comparable to the film width.

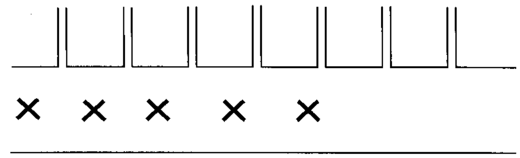

FIG. 9. The regions between adjacent pairs of S probes form cells for PSC's, and a single PSC can nucleate in the middle of each cell. With increasing current, PSC's successively nucleate from left to right, one at a time in a cell. The newest PSC (i.e., the right most one) is likely located to the right side of the cell since there are no PSC's to the right but there are preexisting PSC's to the left and PSC's repel each other. When the next new PSC nucleates, the last PSC will be pushed back toward the center of the cell due to the repulsion of the new PSC now existing to its right. However, the last PSC will still be located to the right of the center of the cell since there are many more PSC's to the left. This allows PSC's to be progressively centered within their respective cells deeper in the W region.

Now we focus on the explanation of the excess voltage and the nonlocal effect in the I-V characteristics in terms of PSC's. The inhomogeneity in our film, together with the presence of S probes, results in the sequential nucleation of individual PSC's in the regions between the S probes. From the measured variation of I_c in the inset in Fig. 3 we can expect that PSC's are nucleated from left to right in our film as the current is increased. If a PSC is already nucleated in a section between the adjacent probes, the section would not host another PSC since the length of the section is shorter than λ_{Q*} and PSC's repel within λ_{Q*} of each other.[32,34] On the other hand, the voltage probes locally enhance the critical current, and so PSC's are unlikely to be found near the probes and instead nucleate between the probes. Thus, the film may be thought of as a 1D array of cells, each of which can contain a PSC in the middle. (See Fig. 9.) As the bias current is increased, a single PSC will successively be nucleated in each cell from left to right (i.e., through sections A–H). The nucleation of a PSC in a section results in the development of a finite voltage in that section. The consecutive appearance of a finite voltage in sections A–H as the current is increased, as shown in Fig. 5, is consistent with the PSC cell picture.

In order to account for the detailed features of the excess voltage, we start with the assumption that PSC's exist to left of probe pair A when we observe the first positive dV/dI peak in the curve A in Fig. 5. The development of a finite voltage indicates a PSC nucleation in cell A (PSC_A). The excess voltage measured with S probes is then due to λ_{Q*} being much greater than the distance between the voltage

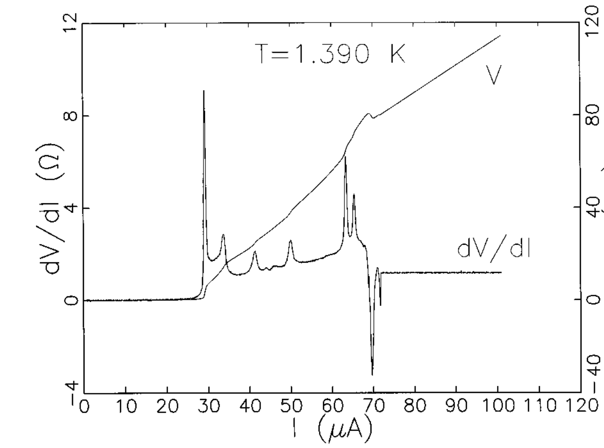

FIG. 10. The dV/dI's (left axis) and I-V characteristics (right axis) measured at $T=1.390$ K across a longer length of the film spanning several probes. The voltage probes are superconducting and located at -12 and 5 μm. The various positive peaks in dV/dI (i.e., incremental increases in voltage) are an indication of the sequential nucleation of PSC's.

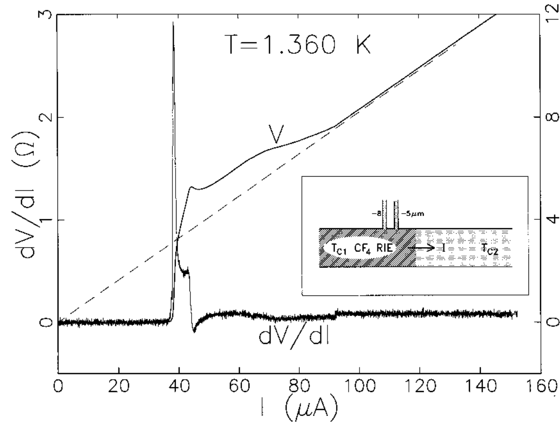

FIG. 11. The dV/dI's (left axis) and I-V characteristics (right axis) of the aluminum film structure with only single pair of S voltage probes. The location of the voltage probes are shown in the inset. Note that the excess voltage is smoothly extinguished. The dashed line is the normal-state I-V characteristics. Inset: The top view of the aluminum film structure with a single pair of S voltage probes, located at -8 and -5 μm from the etched-unetched interface. For the definition of negative positions, see the caption for the inset in Fig. 1. The hashed area represents the region where the T_c is suppressed.

probes, pair A. Since there is no PSC to the right of cell A, it is likely that this PSC_A will be located on the right-hand side of the cell. A further increase in current leads to the introduction of a new PSC in cell B (PSC_B). By symmetry, the nonequilibrium regions between PSC_A and PSC_B must each be confined in cell A and B. Hence, the nucleation of PSC_B leads to the compression of the nonequilibrium region around PSC_A. This can be understood also in terms of a reduction of λ_{Q*} due to the increase in the density of quasiparticles associated with two PSC's. The compression of the nonequilibrium region around PSC_A leads to a decrease in voltage and hence a negative dV/dI. At the same time, PSC_A will be repelled to the left, toward the center of the cell, by the presence of the new PSC in cell B. The sequential introduction of new PSC's to the right of the cell A (as the current is increased) will then lead to a progressive centering of PSC_A in its cell and a progressive confinement of the nonequilibrium region. This produces the incremental decrease in the excess voltage and the nonlocal negative dV/dI peaks associated with the nucleation of new PSC's in the sections between the adjacent voltage probes to the right of the sampled region. In Fig. 10, we see an indication of the existence of PSC's in our film. The steplike increase in voltage is due to the progressive nucleation of PSC's with increasing current. Such behavior has been observed previously.[31,32,35]

We have explained that the sharp features in dV/dI (nonlocal phenomena) are associated with the nucleation of adjacent PSC's which are confined in the sections between the voltage probes and located within λ_{Q*} of each other. The confinement of PSC's is due to the presence of S voltage probes. Thus, a sample similar in all respects but lacking multiple arms of voltage probes should not exhibit the subsequent negative dV/dI features, even though the excess voltage is expected to still be present due to the long λ_{Q*}. In a second experiment, we have fabricated aluminum film structures in a similar manner to the previous experiment, but with only a single pair of S voltage probes located near the etched-unetched interface (see the inset in Fig. 11). In Fig. 11, the I-V characteristics of such a structure demonstrate that the excess voltage is smoothly eliminated over a similar bias current range without the subsequent sharp negative dV/dI features. This is consistent with our prediction.

Other explanations for the anomaly have been given besides the nonequilibrium charge imbalance model. We find that they are inconsistent with our experimental results. Santhanam *et al.*[2] assert that the nonequilibrium model alone is insufficient to explain their observation of a similar anomaly in 1D aluminum wires and suggest that the sample size and dimensionality must play an important role in such behavior. Their explanation appears to be not valid for the reason that the anomaly is also observed in our 2D aluminum systems. Vaglio *et al.*[5] give another explanation: the sample inhomogeneity with out-of-line voltage and current contact configuration produces a resistance peak due to current redistribution effects. Their model is inconsistent with our observation. We find that the manifestation of the anomaly is closely related to the state of the voltage probes (N or S) rather than the probe configuration. Besides, neither of these models can provide an explanation consistent with the nonlocal behavior described in Sec. IV D.

V. ASYMMETRY WITH CURRENT BIAS DIRECTIONS

Finally, we present another interesting observation associated with the excess voltage in our aluminum structures. Figure 12 shows the dV/dI's and I-V characteristics measured with both positive and negative bias currents. The anomaly (i.e., excess voltage) is observed in either current direction. However, there is an asymmetry in the detailed behavior as seen in Fig. 12(a). Whether the measurement is obtained with probes located on the etched or unetched side, or spanning the interface, a similar asymmetry is observed in all the measurements of the dV/dI's in both sample struc-

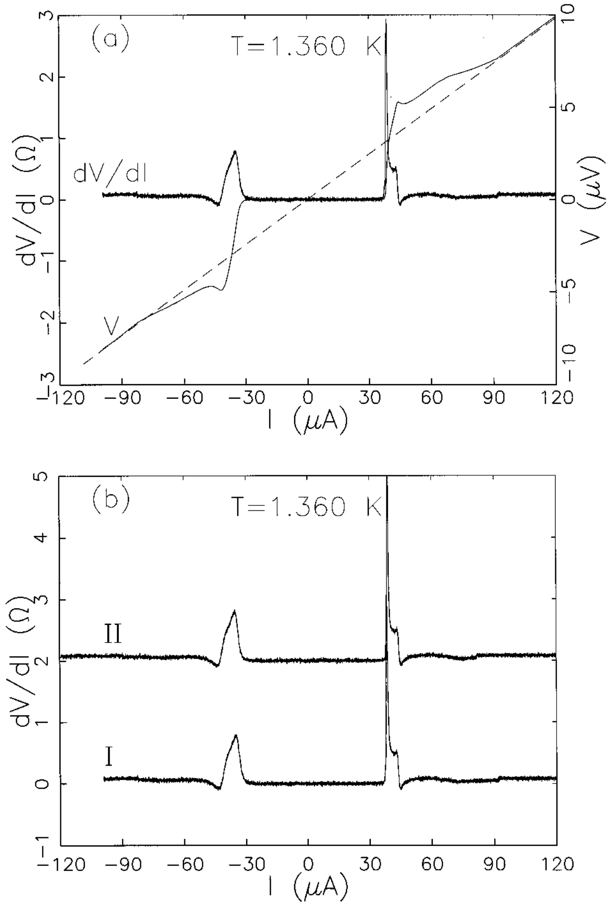

FIG. 12. (a) The dV/dI's (left axis) and I-V characteristics (right axis) are measured with both positive and negative current biases. Note the asymmetry in the shape of the excess voltage with current direction. As an example, we present only the measurements on the aluminum film structure with a single pair of probes. The dashed line is the normal-state I-V characteristic. (b) I: The dV/dI's are measured with an increasing bias current from negative values to zero and then to positive values. II: The dV/dI's are measured with a decreasing bias current from positive values to zero and then to negative values. The trace is shifted with respect to trace I for comparison.

tures with multiple probes as well as with a single pair of probes (see the insets in Figs. 1 and 11). By comparing the two dV/dI traces in Fig. 12(b), it is demonstrated that the asymmetry is nonhysteretic and truly depends on the direction of the current. Whether the bias current is increased from a high negative value to a high positive value or decreased from a high positive value to a high negative value, the same asymmetry in the dV/dI's is reproduced in both cases. If the appearance of the asymmetry were a result of some hysteretic effects, such as local heating, then the behavior of the dV/dI's should have been reversed in the two cases. (The slight discrepancy at high currents is likely due to heating. However, it does not affect the anomaly.)

The nonequilibrium charge imbalance theory[21] does not predict an asymmetry with the current bias directions. We speculate that it is related to the different relaxation times of the charge carriers moving in two different directions. PSC's are always nucleated from left to right according to the I_c gradient shown in the inset in Fig. 3 when the magnitude of the current is increased regardless of its sign. With a negative current, the charge carriers (electrons) move from left to right. However, with a positive current, they move from right to left. Because of the inhomogeneity present in our film, they experience slightly different environments and are thus subjected to different scattering times in the two cases. It is likely that this leads to an asymmetry in the dV/dI with the current bias direction.

VI. CONCLUSION

We have investigated the resistance anomaly and excess voltage in the R vs T and I-V characteristics in 2D aluminum systems with a small T_c variation. The inhomogeneity is produced by the use of the CF_4 RIE technique. Near T_c, we observe an excess voltage and the associated increase in resistance above the normal-state values when the measurements are performed with S voltage probes. We also observe incremental decreases of the excess voltage with increasing bias current, nonlocal effects associated with the nucleation and interaction of PSC's. The main features of these unusual behaviors are explained by the nonequilibrium charge imbalance model which requires differences between the quasiparticle and pair electrochemical potentials to extend over a distance λ_{Q*} in the S region. We discussed a heuristic model that mapped the behaviors seen at an NS interface to that of a WS interface associated with the current-biased states. Though intuitively appealing, this model cannot successfully describe the detailed features in the excess voltage. Finally, we showed that the PSC model is consistent with the observation of an excess voltage as well as the incremental decrease of the excess voltage and the nonlocal phenomena in the I-V characteristics.

It is clear from our study that the origin of the resistance anomaly in our 2D aluminum films is the different spatial gradients of the quasiparticle and pair electrochemical potentials in the superconductor. It is reasonable to expect much of the same physics to be present in other inhomogeneous superconducting systems whether or not the T_c variation is intentionally created. An inhomogeneity of a similar size to our created one is expected to exist naturally in typical experiments (e.g., enhanced superconductivity around a voltage probe, nonuniform film thickness, local defects, etc). We believe that many reported cases of the anomaly should be carefully reexamined on the basis of the nonequilibrium model presented in this paper.

ACKNOWLEDGMENTS

We wish to acknowledge helpful conversations with R. Buhrman, V. Ambegaokar, K. Likharev, M. Tinkham, W. Skocpol, V. Petrashov, and B. Janko. This research was supported by the NSF and Cornell MSC Center under DMR-9121654 and DMR-9016301. Fabrication was carried out at the Cornell Nanofabrication Facility, supported by the NSF under ECS-8619040.

*Present address: Department of Physics, Princeton University, Princeton, NJ 08544.

[1] Y. K. Kwong, K. Lin, P. J. Hakonen, M. S. Isaacson, and J. M. Parpia, Phys. Rev. B **44**, 462 (1991).

[2] P. Santhanam, C. C. Chi, J. Wind, M. J. Brady, and J. J. Bucchignano, Phys. Rev. Lett. **66**, 2254 (1991).

[3] J. J. Kim, J. Kim, H. J. Shin, H. J. Lee, S. Lee, K. W. Park, and E. H. Lee, J. Phys. Condens. Matter **6**, 7055 (1994).

[4] S. Rubin, T. Schimpfke, B. Weitzel, C. VoBloh, and H. Micklitz, Ann. Phys. **1**, 492 (1992).

[5] R. Vaglio, C. Attanasio, L. Maritato, and A. Ruosi, Phys. Rev. B **47**, 15 302 (1993).

[6] M. A. Crusellas, J. Fontcuberta, and S. Pinol, Phys. Rev. B **46**, 14 089 (1992).

[7] A. Nordstrom and O. Rapp, Phys. Rev. B **45**, 12 577 (1992).

[8] E. Spahn and K. Keck, Solid State Commun. **78**, 69 (1991).

[9] H. Vloeberghs, V. V. Moshchalkov, C. Van Haesendonck, R. Jonckheere, and Y. Bruynseraede, Phys. Rev. Lett. **69**, 1268 (1992).

[10] A. W. Kleinsasser and A. Kastalsky, Phys. Rev. B **47**, 8361 (1993).

[11] M. C. de Andrade, Y. Dalichaouch, and M. B. Maple, Phys. Rev. B **48**, 16 737 (1993).

[12] C. Strunk, V. Bruydoncx, C. Van Haesendonck, V. V. Moshchalkov, Y. Bruynseraede, C. J. Chien, and V. Chandrasekhar, Phys. Rev. B **53**, 11 332 (1996).

[13] M. Park, M. S. Isaacson, and J. M. Parpia, Phys. Rev. Lett. **75**, 3740 (1995).

[14] M. L. Yu and J. E. Mercereau, Phys. Rev. B **12**, 4909 (1975).

[15] M. Park, K. R. Lane, J. M. Parpia, and M. S. Isaacson, J. Vac. Sci. Technol. A **13**, 127 (1995).

[16] K. Lin, Y. K. Kwong, M. Park, J. M. Parpia, and M. S. Isaacson, J. Vac. Sci. Technol. B **9**, 3511 (1991).

[17] J. Clarke, Phys. Rev. Lett. **28**, 1363 (1972).

[18] S probes contacting an N region would always measure the quasiparticle electrochemical potential since the pair electrochemical potential is not defined when the film is in the N state. In a superconductor below its T_c but with a current larger than I_c, the pair electrochemical potential is still not equal to the quasiparticle electrochemical potential [e.g., Dolan and Jackel (Ref. 33)]. Since the electrodes are superconducting and do not carry a current, the pair electrochemical potential must be constant in the superconductor whether in the main strip or the probes.

[19] In the result of Santhanam *et al.* (Ref. 2), the film was homogeneous but so narrow as to affect T_c. Thus, the presence of voltage probes itself led to an enhancement of T_c and created NS interfaces across the entire film. We have carried out measurements on films down to 5 μm in width and in all cases we see similar result.

[20] For the film with a single pair of probes, $T_{c1}=1.363$ K and $T_{c2}=1.406$ K. For both etched and unetched regions, the normal-state resistivity, diffusion constant, elastic mean free path, the residual resistance ratio, and the coherence length are ~ 1.4 $\mu\Omega$ cm, ~ 60 cm^2/s, ~ 130 Å, ~ 2.9, and ~ 1 μm, respectively.

[21] J. Clarke, in *Nonequilibrium Superconductivity*, edited by D. N. Langenberg and A. I. Larkin (North-Holland, Amsterdam, 1986), and references therein.

[22] T. M. Klapwijk and J. E. Mooij, Phys. Lett. **57A**, 97 (1976).

[23] C. C. Chi and J. Clarke, Phys. Rev. B **19**, 4495 (1979).

[24] M. Stuivinga, C. L. G. Ham, T. M. Klapwijk, and J. E. Mooij, J. Low Temp. Phys. **53**, 633 (1983).

[25] P. G. de Gennes, *Superconductivity in Metals and Alloys* (Benjamin, New York, 1966).

[26] Y. K. Kwong, K. Lin, M. Park, M. S. Isaacson, and J. M. Parpia, Phys. Rev. B **45**, 9850 (1992).

[27] In the previous work (Ref. 26), the observed effect was identified as a long-range proximity effect, which is an equilibrium phenomenon, under the assumption that measurements were free from complication by nonequilibrium effects associated with NS interfaces. However, the validity of the assumption may be questionable, and we believe that the data need to be reanalyzed with a possibility of the presence of nonequilibrium effects in mind. Even though the observed long-range effect by itself is quite interesting, the investigation of its mechanism is beyond the scope of this paper, and we limit our discussion to the resistance anomaly. What is relevant to our discussion is the existence of a long-range variation of the T_c in inhomogeneous aluminum film structures fabricated by the use of the RIE technique (Ref. 15).

[28] A complete treatment should account for the presence of the equilibrium proximity effect as well as the nonequilibrium charge imbalance. Since $\lambda_{Q*} > \xi(T)$, we have neglected the proximity effect in this discussion.

[29] At these temperatures, the nonequilibrium charge imbalance length will be much smaller than the length of the voltage probes (many hundreds of microns), and so there can be no ambiguity that the probes register the pair electrochemical potential even if there exists a nonequilibrium at the probe junction. Also see the remark in Ref. 18. Furthermore we note that in the zero-current-biased state similar resistance anomalies are observed with S (unetched) probes regardless of whether a NS interface is present at the probe junction (when the film is etched) or when the NS interface is most likely away from the junction as in the case when the film is unetched. Therefore, the presence of an $N(W)$-S interface at the voltage probe junctions to the current carrying main strip is unlikely to be the source of the phenomena observed in this experiment.

[30] J. S. Langer and V. Ambegaokar, Phys. Rev. **164**, 498 (1967).

[31] J. M. Aponte and M. Tinkham, J. Low. Temp. Phys. **51**, 189 (1983).

[32] W. J. Skocpol, M. R. Beasley, and M. Tinkham, J. Low. Temp. Phys. **16**, 145 (1974).

[33] G. J. Dolan and L. D. Jackel, Phys. Rev. Lett. **39**, 1628 (1977).

[34] M. Tinkham, J. Low. Temp. Phys. **35**, 147 (1979).

[35] J. Meyer and G. von Minnegerode, Phys. Lett. **38A**, 529 (1972).